

# UCSF

## UC San Francisco Previously Published Works

### Title

The conserved arginine 380 of Hsp90 is not a catalytic residue, but stabilizes the closed conformation required for ATP hydrolysis

### Permalink

<https://escholarship.org/uc/item/29b972hb>

### Journal

Protein Science, 21(8)

### ISSN

0961-8368

### Authors

Cunningham, Christian N  
Southworth, Daniel R  
Krukenberg, Kristin A  
et al.

### Publication Date

2012-08-01

### DOI

10.1002/pro.2103

Peer reviewed

# The conserved arginine 380 of Hsp90 is not a catalytic residue, but stabilizes the closed conformation required for ATP hydrolysis

Christian N. Cunningham,<sup>1,2</sup> Daniel R. Southworth,<sup>2</sup> Kristin A. Krukenberg,<sup>2,3</sup> and David A. Agard<sup>2\*</sup>

<sup>1</sup>Graduate Group in Biophysics, University of California, San Francisco, California 94158

<sup>2</sup>Department of Biochemistry and Biophysics, Howard Hughes Medical Institute, University of California, San Francisco, California 94158

<sup>3</sup>Graduate Program in Chemistry and Chemical Biology, University of California, San Francisco, California 94158

Received 6 March 2012; Revised 22 May 2012; Accepted 23 May 2012

DOI: 10.1002/pro.2103

Published online 31 May 2012 proteinscience.org

**Abstract:** Hsp90, a dimeric ATP-dependent molecular chaperone, is required for the folding and activation of numerous essential substrate “client” proteins including nuclear receptors, cell cycle kinases, and telomerase. Fundamental to its mechanism is an ensemble of dramatically different conformational states that result from nucleotide binding and hydrolysis and distinct sets of interdomain interactions. Previous structural and biochemical work identified a conserved arginine residue (R380 in yeast) in the Hsp90 middle domain (MD) that is required for wild type hydrolysis activity in yeast, and hence proposed to be a catalytic residue. As part of our investigations on the origins of species-specific differences in Hsp90 conformational dynamics we probed the role of this MD arginine in bacterial, yeast, and human Hsp90s using a combination of structural and functional approaches. While the R380A mutation compromised ATPase activity in all three homologs, the impact on ATPase activity was both variable and much more modest (2–7 fold) than the mutation of an active site glutamate (40 fold) known to be required for hydrolysis. Single particle electron microscopy and small-angle X-ray scattering revealed that, for all Hsp90s, mutation of this arginine abrogated the ability to form the closed “ATP” conformational state in response to AMPPNP binding. Taken together with previous mutagenesis data exploring intra- and intermonomer interactions, these new data suggest that R380 does not directly participate in the hydrolysis reaction as a catalytic residue, but instead acts as an ATP-sensor to stabilize an NTD-MD conformation required for efficient ATP hydrolysis.

**Keywords:** Hsp90; conformational dynamics; catalysis; interactions; ATP hydrolysis

---

Additional Supporting Information may be found in the online version of this article.

Christian N. Cunningham and Daniel R. Southworth contributed equally to this work.

Christian N. Cunningham's current address is Early Discovery Biochemistry, Genentech, Inc., 1 DNA Way, MS27, South San Francisco, CA 94080.

Daniel R. Southworth's current address is Department of Biological Chemistry, Life Sciences Institute, University of Michigan, 210 Washtenaw Ave, Ann Arbor, MI 48109.

Kristin A. Krukenberg's current address is Department of Systems Biology, Harvard Medical School, 200 Longwood Ave, Warren Alpert 536, Boston, MA 02115.

Grant sponsor: UC Discovery Grant; Grant number: bio03-10401/Agard; Grant sponsor: NIH; Grant number: T32 GM08284; Grant sponsor: ACS Postdoctoral Fellowship; NSDEG Graduate Fellowship; Howard Hughes Medical Institute; ARCS Fellowship.

\*Correspondence to: Dr. David A. Agard, 600 16th St., MC2240 Room S412D, San Francisco, CA 94158. E-mail: agard@msg.ucsf.edu

## Introduction

Hsp90 is a member of the molecular chaperone family of proteins that facilitate protein folding in the cell. Well-characterized chaperones including Hsp60 (GroEL/ES) and Hsp70 (DnaK) promote protein folding by discrete cycles of ATP hydrolysis-driven binding and release of nascent polypeptides and exposed hydrophobic regions.<sup>1</sup> However, unlike those family members, Hsp90 acts much later in the folding process, interacting with a specific set of client proteins in a near-native state conformation and promoting conformational rearrangements required for ligand binding and downstream signaling events.<sup>2–7</sup> In eukaryotes, these client proteins include many signaling and regulatory proteins such as serine/threonine and tyrosine kinases, telomerase, steroid hormone receptors, and tumor suppressor proteins.<sup>8–11</sup> The importance of these client proteins in signaling and cellular function has made Hsp90 an attractive target for anticancer therapeutics.<sup>12</sup> A majority of the drugs that inhibit Hsp90 function target the ATP binding pocket underscoring the importance of ATP hydrolysis in its chaperoning activity.<sup>13,14</sup> Although nucleotide hydrolysis has been shown to be absolutely required for the *in vivo* chaperone function of Hsp90<sup>15,16</sup> how the energy from ATP binding and hydrolysis contributes to both chaperone conformational changes and client activation remains largely unknown.

Hsp90 is a constitutive dimer where each ~90 kDa monomer consists of three domains: the N-terminal nucleotide-binding domain (NTD), the middle domain (MD), and the C-terminal dimerization domain (CTD). Hsp90 domain structures,<sup>17–19</sup> comparisons with other GHKL superfamily members such as MutL and GyrB,<sup>17,19–21</sup> and Hsp90 truncation studies concluded that the Hsp90 NTD provides all of the structural requirements for nucleotide binding<sup>5,17,22</sup> and a conserved catalytic glutamate which activates the attacking water in the ATP hydrolysis reaction<sup>23</sup> [Fig. 1(c)]. However, the NTD alone is not sufficient for ATP hydrolysis, the MD is required for even minimal activity and full activity requires both the MD and dimerization.<sup>5</sup>

The availability of full-length crystal structures of the bacterial (apo and ADP states)<sup>24</sup> and yeast Hsp90 (using the nonhydrolyzable ATP analog, AMPPNP)<sup>25</sup> provided important insights into the relationships between domain structure, organization, and ATPase activity. The structures revealed dramatically different conformational states that are stabilized by different interactions, each with varying degree of exposure of conserved hydrophobic patches on the chaperone, in response to nucleotide binding [Fig. 1(a)],<sup>24,25</sup> suggesting an allosteric coupling between nucleotide and conformational states. Single particle EM studies confirmed that these three conformational states (apo, ATP, ADP) are uni-

versally conserved across bacterial, yeast, and human Hsp90s.<sup>26</sup> By contrast, analysis of individual Hsp90 molecules by EM and population averages by SAXS revealed that AMPPNP or ADP binding does not trigger a discrete conformational change but rather shifts a preexisting equilibrium of states toward the appropriate conformation.<sup>26–28</sup>

Kinetic studies on Hsp90 homologs from different species demonstrated that the chaperone is a very slow ATPase with activities ranging from 0.1 (human) to 1.2 (yeast) pmol/min/pmol<sup>18,19</sup> although this can be altered by client binding.<sup>29–31</sup> Data from yeast mutants suggests that ATPase rates are precisely tuned for each organism, as even small increases or decreases in ATPase rates (T22I 7-fold increase; T101I 3-fold decrease) will compromise growth ability.<sup>16</sup> From enzyme kinetics, it appears that the chemical ATP hydrolysis step is orders of magnitude faster than domain closure, indicating that conformational changes are rate-limiting.<sup>32</sup> This is supported by an observed cross-species correlation between ATPase rates and the population of closed states in the presence of AMPPNP<sup>26</sup> as well as by direct kinetic observation of domain closure by either FRET or small angle x-ray scattering (SAXS).<sup>27,28</sup> Given the apparent contradiction between the required precision of ATPase rates for *in vivo* function and the rather weak coupling between nucleotide and conformation observed *in vitro*, we wished to further probe the molecular basis for nucleotide recognition, hydrolysis, and chaperone conformation.

Initially identified by comparison with GHKL family members,<sup>33–35</sup> arginine 380 in the yeast Hsp82 MD (referred to as Arg<sub>MD</sub> to simplify cross species comparisons), was shown to have a significant role in ATP hydrolysis (related to Lys 307 of MutL and Lys 33 of GyrB). Mutation of this residue in Hsp90 resulted in a decrease in ATP hydrolysis *in vitro* and a loss of viability *in vivo*,<sup>19</sup> leading to the suggestion that Arg<sub>MD</sub> is a catalytic residue directly participating in the activation and chemistry of the hydrolysis reaction. The crystal structure of Hsp82 in complex with AMPPNP and the co-chaperone Sba1 supported this hypothesis, revealing a direct interaction between the Arg<sub>MD</sub> and the AMPPNP  $\gamma$ -phosphate in the closed state [Fig. 1(c)].<sup>25</sup> By contrast, the *E. coli* apo N-M structure, Grp94 N-M structures, and the yeast MD structures (PDB: 1Y4U, 2O1W, 1HK7) all show a direct interaction of Arg<sub>MD</sub> with an exposed and conserved loop on the MD stabilizing the apo state of Hsp90 [Fig. 1(b)].

Previous work from our lab indicated that Arg<sub>MD</sub> does not act alone in the activation of ATP hydrolysis but rather is involved synergistically with a network of residues from both monomers to

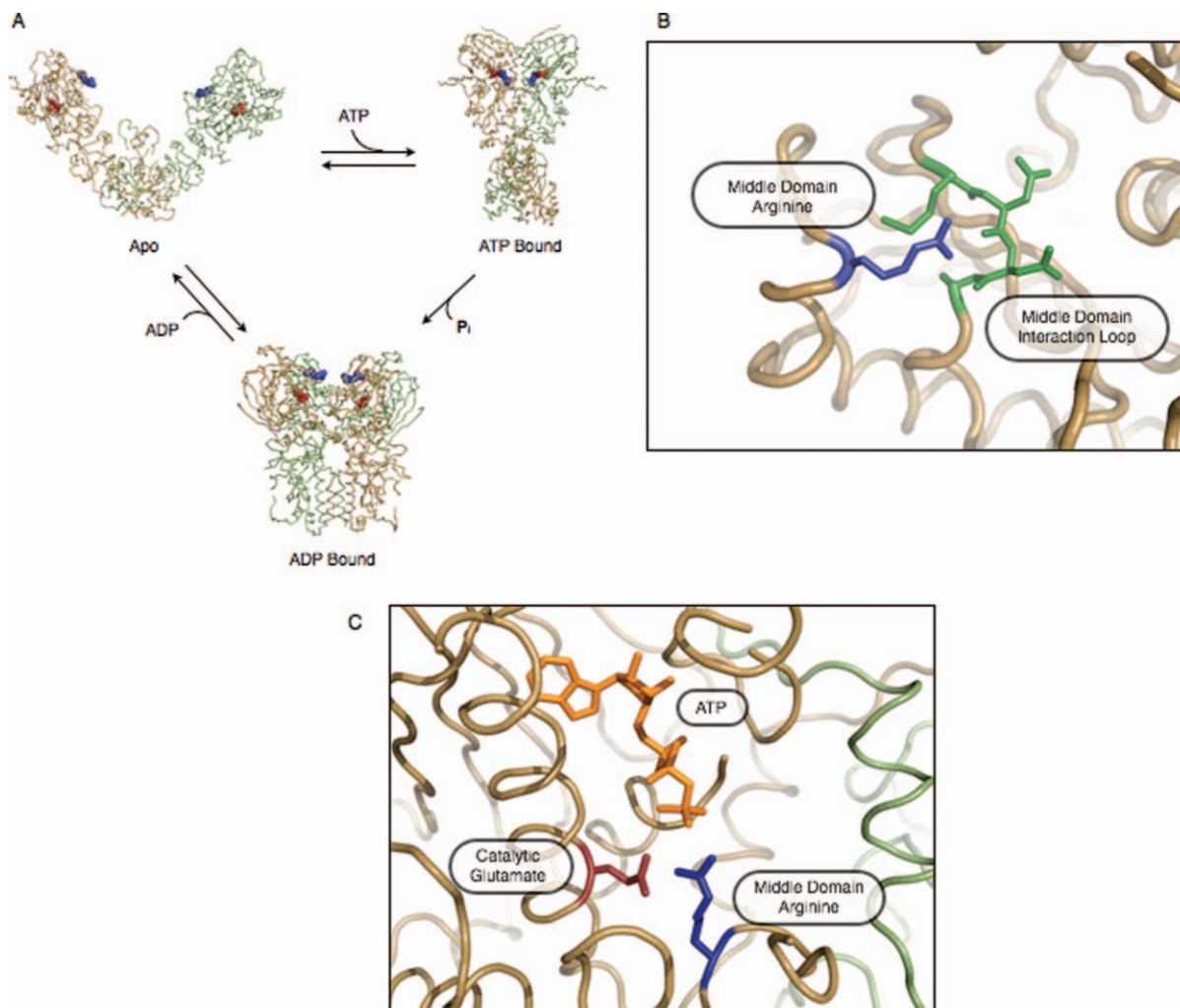


**Figure 1.** Hsp90 undergoes nucleotide-dependent conformational rearrangements. (A) Previous crystallographic studies show that the conformational equilibrium of Hsp90 is biased by nucleotide binding and results in large changes in quaternary structure. The catalytic glutamate (blue) and middle domain arginine (red) are highlighted in each structure (apo and ADP conformation are bacterial; AMPPNP bound is yeast) showing these residues only coming together in the AMPPNP bound closed state completing a hydrolysis competent active site. (B) Close-up view of the bacterial middle domain of the apo state. The Arg<sub>MD</sub> (blue) interacts with a conserved loop (green) on this middle domain which must be released for the closed state to occur. (C) Close-up view of the nucleotide binding pocket in the yeast AMPPNP bound closed state. The catalytic glutamate (red) orients the attacking water in the hydrolysis reaction while the Arg<sub>MD</sub> (blue) interacts with the gamma phosphate of AMPPNP (orange) acting as a nucleotide sensor.

stabilize a hydrolysis competent Hsp90 conformation.<sup>36</sup> While investigating this network of interactions we discovered that the equivalent Arg to Ala mutation in *E. coli* (R336A) had an unexpectedly mild effect raising questions about the true role of this important residue, and indicating that further investigation was required.

## Results

### ***Hydrolysis rates of the middle domain arginine indicate a noncatalytic role in ATP hydrolysis***

Arg<sub>MD</sub> was mutated to an alanine in the bacterial (HtpG•R336A), yeast (Hsc82•R376A), and human (Hsp90 $\alpha$ •R400A) Hsp90 homologs and ATP hydroly-

sis rates were measured by release of radioactive inorganic phosphate. Previous work has shown that the affinity of ATP for the NTD alone is essentially unchanged when compared to the full-length protein (132  $\mu$ M vs. 172  $\mu$ M, respectively), thus residues in the MD, including the Arg<sub>MD</sub>, do not contribute significantly to nucleotide binding.<sup>15,17</sup> The Hsp90-specific inhibitor, geldanamycin, was used to control for any small amounts of contaminating ATPases (see Methods). Mutation of Arg<sub>MD</sub> resulted in a decreased ATPase rate in all species, with yeast showing the most severe effect (a seven-fold reduction) (Fig. 2; Table I). By contrast, the human and bacterial Hsp90s, showed only marginal (approximately two-fold) losses in activity when compared to

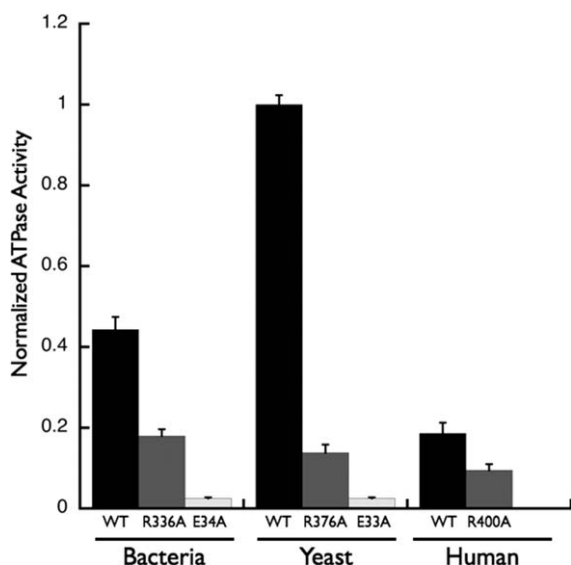


**Figure 2.** ATP hydrolysis rates of the bacterial, yeast, and human Hsp90 homologs. Bacterial, yeast, and human homologs of Hsp90 were mutated and assayed for ATP hydrolysis. Wild type rates are shown in black; arginine mutant rates are shown in gray; catalytic glutamate mutants are shown in white. All measured hydrolysis rates were normalized to the wild type yeast homolog rate. The Arg<sub>MD</sub> shows a substantial defect in ATP hydrolysis that was not consistent among all three homologs tested and was not as deleterious to activity as the catalytic glutamate in all three cases.

their respective wild-type constructs. Given the very high levels of sequence and structural conservation, this was quite unexpected, although these results are comparable to those observed for mutations of the homologous residue in MutL, Lys 307.<sup>33</sup> To ensure that we were mutating the homologous Arg<sub>MD</sub> between species we mutated and measured the ATP hydrolysis rates of several positively charged residues surrounding Arg<sub>MD</sub> in the bacterial homolog. These mutations displayed no change in ATP hydrolysis (data not shown) when compared to the wild-type rate indicating that the originally mutated residues were indeed functionally homologous equivalents to Arg336 in yeast. Thus while Arg<sub>MD</sub> is important for maintaining wild-type levels of ATPase activity and yeast viability, the very mild affects observed in both the human and bacterial enzymes indicate that this residue is not essential for the ATPase reaction.

As a control for species/variant differences, we measured the ATP hydrolysis rates of the bacterial and yeast homologs with the known catalytic glutamate mutated to an alanine (Hsc82•E33A and HtpG•E34A); due to the very low ATPase basal activity of human Hsp90 and the known conserved catalytic role the respective catalytic glutamate mutation was not made. As expected, the bacterial and yeast mutants were both severely compromised (17-

and 40-fold reductions, respectively) with almost no ATP hydrolysis measured above the noise level of this experiment (Fig. 2; Table I). These data support the known conserved role of the glutamate in the GHKL family of enzymes coordinating the attacking water in the hydrolysis reaction.<sup>15,21,23,33–35</sup> Thus, with such a large discrepancy between the hydrolysis rates of the arginine and the glutamate mutations observed with both homologs and the overall modest loss in activity of the Arg<sub>MD</sub> mutants, our results suggest that the Arg<sub>MD</sub> is not required for catalysis, but instead plays an indirect role in promoting ATP hydrolysis.

### **Solution X-ray scattering suggests Arg<sub>MD</sub> is important for conformational stabilization**

We next sought to better define the role of Arg<sub>MD</sub>. From crystal structures it is clear that the arginine residue adopts distinct local interactions in the apo and ATP states [Fig. 1(b,c)] that appears to stabilize Hsp90 into one conformation or the other. Given the unique arrangement of Arg<sub>MD</sub> in the closed state, an alternative role could be to stabilize a hydrolysis-competent Hsp90 conformation in an ATP-specific manner. To test this, we performed small angle X-ray scattering (SAXS) on the bacterial and yeast wild type and mutant constructs in the presence and absence of AMPPNP. Previous fluorescence studies have shown that the nonhydrolyzable analog of ATP, AMPPNP, is able to stabilize the same conformation of Hsp90 as ATP and is utilized in these structural studies to prevent conformational cycling of Hsp90.<sup>28,32</sup>

Experimental scattering intensity curves ( $I(q)$ ) of each homolog were measured in the presence and absence of nucleotide and transformed into interatomic probability profiles,  $P(r)$ , providing information on the overall molecular shape (Fig. 3; left column). In both wild-type homologs, the apo state shows a broad distribution of distances in the  $P(r)$  curves representing the very extended open conformation populated in the absence of nucleotide.<sup>27</sup> With the addition of saturating amounts of AMPPNP the bacterial and yeast SAXS curves exhibit a more narrow range of distances in their  $P(r)$  curves with a peak around 55 Å indicating a

**Table I.** ATP Hydrolysis Rates for Hsp90 Homologs and Mutants

Organism	Wild-type <sup>a</sup>	Arginine mutant <sup>a</sup>	Glutamate mutant <sup>a</sup>
Bacteria	0.52 ± 0.06	0.21 ± 0.03	0.03 ± 0.005
Yeast	1.2 ± 0.05	0.16 ± 0.04	0.03 ± 0.005
Human	0.21 ± 0.05	0.11 ± 0.03	N/A
Yeast N599	0.14 ± 0.02	0.05 ± 0.01	0.008 ± 0.005

<sup>a</sup> Hydrolysis rates are reported as pmol ATP hydrolyzed/min/pmol protein.

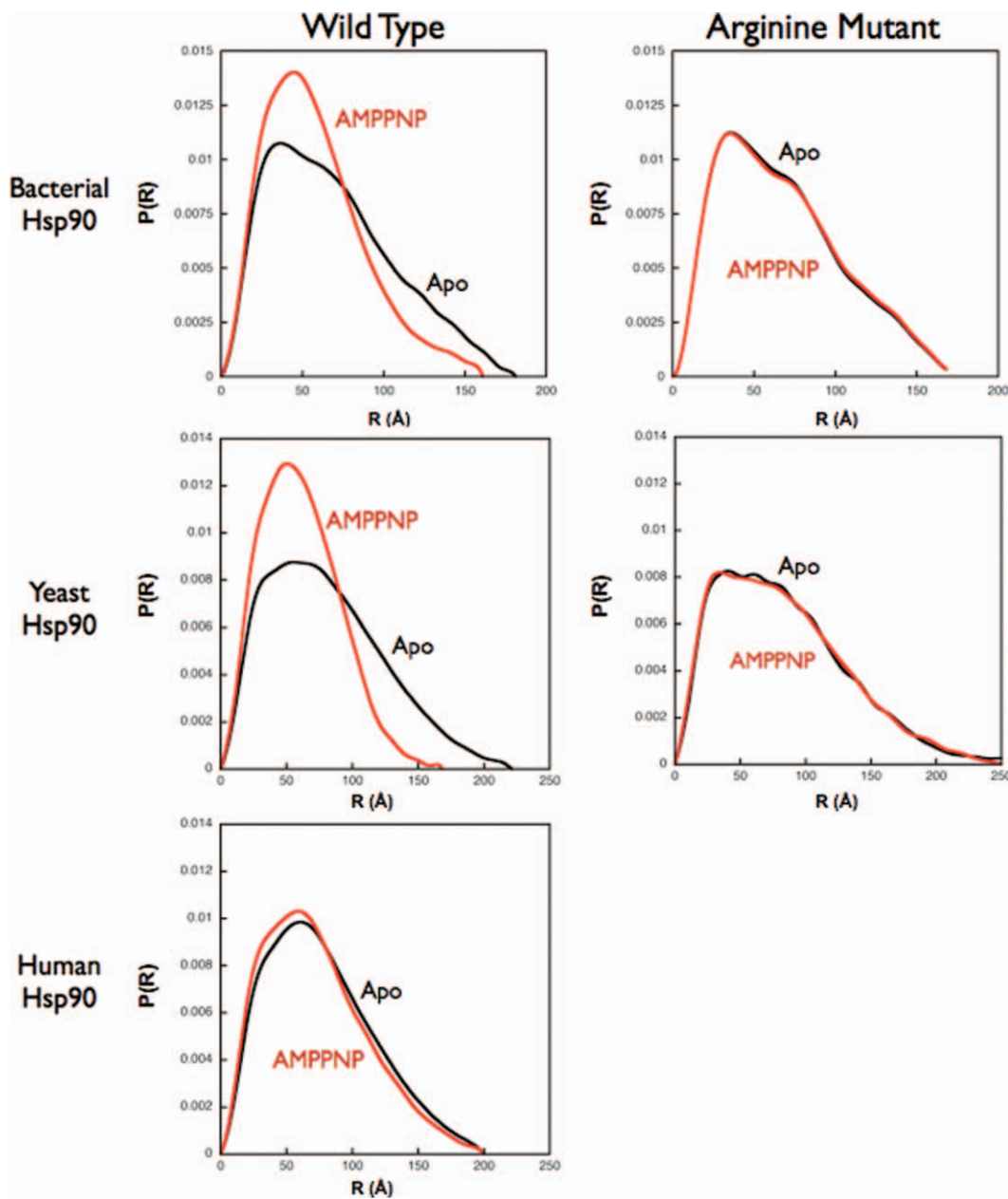


**Figure 3.** SAXS analysis on the middle domain arginine mutants. Small-angle X-ray scattering was used to investigate whether the Arg<sub>MD</sub> affects the conformational equilibrium of the bacterial, yeast, and human Hsp90 homologs.  $P(r)$  curves for the wild type (left) and mutant (right) proteins under apo conditions are colored in black; AMPPNP bound curves are colored red. Solution scattering of both the bacterial and yeast proteins confirm the results obtained using electron microscopy.

more closed compact state of Hsp90. Beyond providing qualitative shape information, the  $P(r)$  profiles can be quantitatively fit to accurately determine Hsp90 conformations or to extract the relative populations of different conformational states.<sup>27</sup>

In the absence of nucleotide, the  $P(r)$  curves are essentially identical for the *E. coli*, yeast, and Arg<sub>MD</sub> mutants (Fig. 3; right column). However, upon nucleotide addition neither mutant displayed the conformational shift observed in the wild-type proteins indicating that the closed state is not being

formed in solution. Because the conformational equilibrium of wild-type human Hsp90 vastly favors the open state under saturating AMPPNP,<sup>26</sup> it was not productive to pursue SAXS measurements for the human arginine mutant (Fig. 3; bottom row).

**Electron microscopy confirms the middle domain arginine stabilizes the closed state of Hsp90**

In support of the solution X-ray scattering data and to surmount the challenges in evaluating the effects

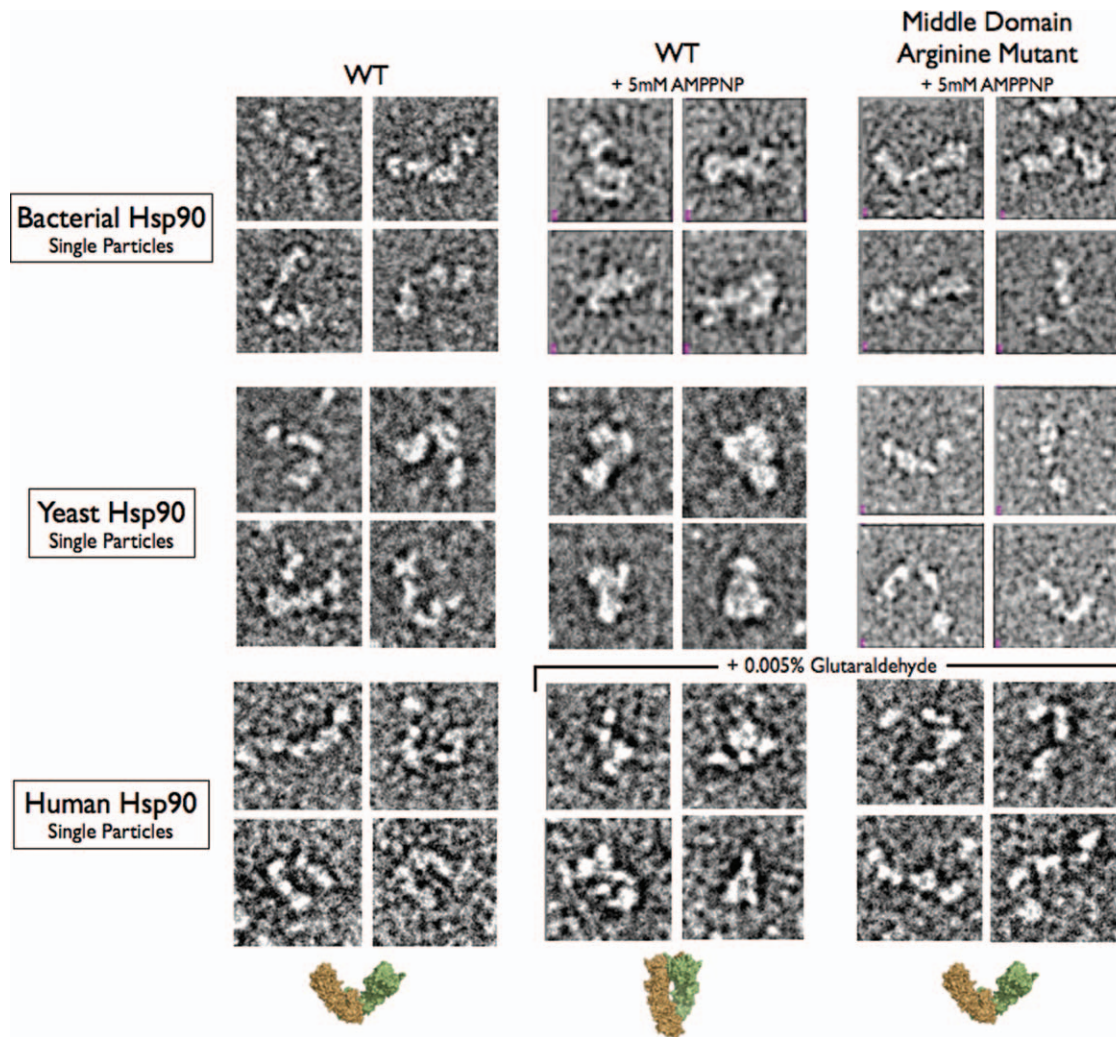


**Figure 4.** Electron microscopy single particle analysis of bacterial, yeast, and human Hsp90. Electron microscopy was used to confirm that the conformational defect observed in solution. Wild type proteins of all homologs displayed the canonical dynamic open state conformations under apo conditions (left column) and the closed, N-terminal dimerized conformation when saturating amounts of AMPPNP were added to the solution (middle column). The human protein required the addition of 0.005% glutaraldehyde to detect the closed state in the presence of AMPPNP. In contrast, the arginine mutants of all three homologs show an inability to stabilize the closed state in the presence of AMPPNP (right column).

of the Arg<sub>MD</sub> to Ala mutation on the human Hsp90, we used single particle negative stain electron microscopy<sup>37</sup> of the wild-type and mutant arginine in all three Hsp90 homologs in the presence and absence of the nonhydrolyzable ATP analog, AMPPNP. In the absence of nucleotide, the bacterial, yeast, and human homologs show a wide range of open angles between the two monomers similar to what was observed in our previous electron microscopy and SAXS studies (Fig. 4, Supporting Information Fig. 1).<sup>26,27</sup> As observed previously,<sup>26</sup> upon the addition of AMPPNP the majority of the bacterial and yeast Hsp90s form the closed state with the NTDs dimerized in a conformation equivalent to that seen in the Hsp82:Sba1:AMPPNP crystal structure.<sup>25</sup> While HtpG•R336A and Hsc82•R376A looked identical to the wild-type under apo condi-

tions (data not shown), no conversion to the closed state was observed upon the addition of 5 mM AMPPNP.

As seen with the human Hsp90 solution scattering results, the closed state is only transiently sampled despite the presence of saturating amounts of AMPPNP. Therefore, to address this, we added a small amount of glutaraldehyde crosslinker, as previously reported,<sup>26</sup> to trap the closed state in a nucleotide-dependent manner for visualization (Fig. 4, Supporting Information Fig. 2). Following crosslinking, the closed state was not readily observed for human Hsp90•R400A in the presence of AMPPNP, while the wild type particles appeared closed and similar to HtpG and yeast under the same conditions. Thus, while the effects of this mutation on ATPase rates are modest and

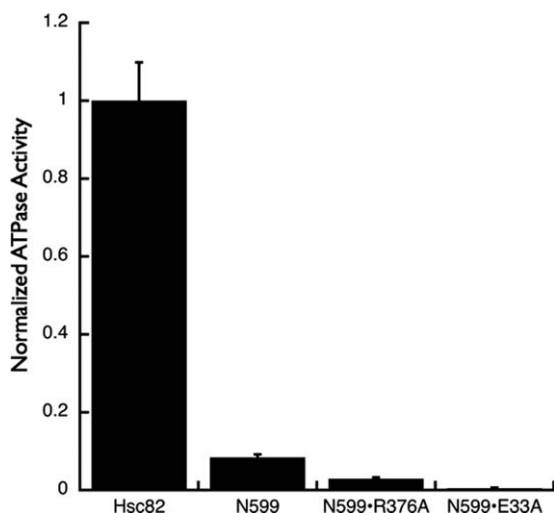


**Figure 5.** Middle domain arginine is directly involved in stabilizing an N-middle conformation that is competent for hydrolysis. Normalized ATPase activities of the yeast Hsp90 homolog, C-terminal truncation (N599), and the arginine and glutamate mutants in the C-terminal truncation construct. There is a substantial loss of activity observed when C-terminal dimerization is removed. A further loss of activity is seen when the arginine is mutated indicating its role in stabilizing a hydrolysis competent conformation of the N-middle domains. The glutamate mutant in the N599 construct shows no detectable activity as predicted from the full length activities.

variable, our EM and SAXS results indicate a conserved and significant effect on closed conformation of Hsp90.

#### **The middle domain arginine affects N-M domain dynamics**

While mutation of Arg<sub>MD</sub> to an alanine blocks the ability to efficiently form the closed, NTD-dimerized state, it was unclear if Arg<sub>MD</sub> could directly stabilize an ATP hydrolysis competent NTD-MD conformation, or rather acted along only in the context of synergistic intersubunit interactions<sup>36</sup> that together support the closed NTD-dimerized state. To test this, we explored the Arg<sub>MD</sub>-Ala mutation in the context of a yeast Hsp90 construct lacking the CTD dimerization domain (Hsc82•N599). *In vitro*, Hsc82•N599 is a monomer in solution and shows an ~10-fold reduction in ATP hydrolysis (Fig. 5) agreeing with data published previously for Hsp82.<sup>5</sup> As expected from the full-length results, when the catalytic glutamate was mutated to alanine in the truncated construct no activity could be measured. Upon mutation of Arg<sub>MD</sub>, ATPase activity decreased three-fold indicating that this arginine helps to stabilize a hydrolysis-competent NTD-MD conformation even in the absence of NTD dimerization. Notably, the activity of the Ala mutant in the full-length protein is greater than the wild type N599 construct suggesting transient N-terminal dimeriza-

tion and ATP hydrolysis in the full-length protein must be occurring even though it is below the detection threshold of our structural assays. This is supported by the contribution of cross-monomer residues to ATP hydrolysis, even in the context of the Arg<sub>MD</sub> mutant.<sup>36</sup>

#### **Discussion**

ATP hydrolysis and the conformational changes that are coupled to this catalytic cycle are central to the function of Hsp90 by providing the energy to bind, remodel, and release substrate client proteins. Although structural studies have shown that all homologs of Hsp90 appear to undergo similar conformational changes in the presence of nucleotide, there are substantial species-dependent differences in the conformational equilibria and kinetics. Mutations made in yeast Hsp82 that either subtly enhance or decrease ATP hydrolysis showed substantial growth defects indicating that ATPase rates and the conformational equilibrium are highly optimized for the specific function of each homolog *in vivo*.<sup>16</sup>

To better understand how conformational equilibria and ATP hydrolysis are coupled and to determine if there is a universal mechanism among Hsp90 homologs despite the notable differences, we explored the role of the completely conserved Arg<sub>MD</sub> in the bacterial, yeast, and human Hsp90 homologs. As shown here, the large impact of mutating Arg<sub>MD</sub> to Ala on ATPase rate previously observed for yeast Hsp90, appears to be exclusive to yeast, with only two fold decreases observed with either the bacterial or human enzymes. This mild and variable contribution of Arg<sub>MD</sub> to ATP hydrolysis rates suggests that it does not make a critical contribution to chemical hydrolysis as expected for a conserved catalytic residue.

By contrast, electron microscopy and SAXS both indicated that Arg<sub>MD</sub> does play a conserved role in stabilizing the closed state in the presence of AMPPNP. Additionally, mutation of Arg<sub>MD</sub> has a significant affect on the ATPase activity of a monomeric yeast NTD-MD construct lacking the C-terminal dimerization domain. Together these data indicate that Arg<sub>MD</sub> must contribute directly to stabilization of a catalysis-competent NTD-MD conformation, independent of NTD dimerization. The importance of setting of a defined NTD-MD conformation is underscored by the recent discovery that a novel class of inhibitors that bind at this interface show both selectivity for nucleotide state and function by only inhibiting the binding of specific subsets of client and cochaperone interactions.<sup>38,39</sup>

While attention has focused on interaction of Arg<sub>MD</sub> with the  $\gamma$ -phosphate of ATP, several apo Hsp90 crystal structures reveal that Arg<sub>MD</sub> directly interacts with a conserved MD loop in the apo



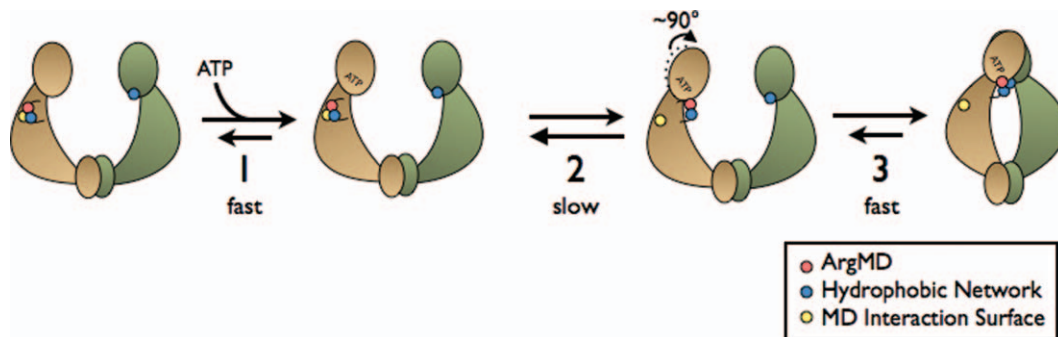


**Figure 6.** Model. Stabilization of the hydrolysis competent state of Hsp90 requires a synergistic set of interactions between the N-terminal domains, a cross monomer hydrophobic network (blue), and the release of the Arg<sub>MD</sub> from the MD to interact with the gamma-phosphate of ATP (yellow and red). In the apo state the Arg<sub>MD</sub> loop interacts with a conserved loop on the MD. Upon ATP binding (Step 1) the NTD the Arg<sub>MD</sub> is released from the MD interaction loop and in combination with a  $\sim 90^\circ$  rotation of the NTD-MD interface can interact with the gamma-phosphate of ATP (Step 2) and stabilize the hydrolysis competent state of Hsp90 (Step 3). We propose that the conformational switching of the Arg<sub>MD</sub> loop and the rotation of the NTD-MD domains are slow in comparison to ATP binding and NTD (Step 3).

state.<sup>19,40,41</sup> Thus some of the functional importance of Arg<sub>MD</sub> may come from its ability to also stabilize the apo conformation. From this structural data and the work presented here we propose a model where these stabilizing MD interactions in the apo state (Fig. 6; yellow region) must first be released followed by a  $\sim 90$  degree rotation of the N-M domain<sup>42</sup> in order for NTD dimerization and subsequently ATP hydrolysis to occur. We propose that release of these constraints and sampling the N-M rotated conformation may actually represent the rate limiting steps in the ATP hydrolysis cycle (Fig. 6; step 2) whereas ATP binding, NTD closure and chemical hydrolysis are comparatively fast.<sup>32</sup> Thus Arg<sub>MD</sub> may be playing a role in slowing the forward reaction by stabilizing the apo state while even more significantly slowing the rate of NTD rotation and re-opening by recognizing the ATP  $\gamma$ -phosphate. From current and previous work<sup>36</sup> we know that the closed and catalytically active conformation is synergistically stabilized by a combination of the Arg interactions, a cross-monomer hydrophobic interaction network, and the NTD dimerization interface.

Together this work shows that although Arg<sub>MD</sub> directly interacts with the  $\gamma$ -phosphate, its primary role is as an ATP sensor that acts to stabilize a specific NTD-MD conformation rather than playing a direct catalytic role in the hydrolysis reaction. We also show that this mechanism of action is universal among a broad array of Hsp90 homologs even though ATP hydrolysis rates and conformational equilibria of the individual species vary greatly. In conjunction with previous work,<sup>36</sup> it is now apparent that the ATPase active conformation is stabilized by an array of interdomain and intersubunit interactions that include, but are not limited to NTD dimerization that ultimately act to tune the rates of to

match the *in vivo* requirements for chaperone function.

## Materials and Methods

### Hsp90 homolog purification

All three proteins were purified in a similar manner. Bacterial and yeast protein was purified from induced *E. coli* cultures using Ni-NTA affinity resin (Qiagen), followed by anion exchange and size exclusion chromatography on a Superdex S200 column (GE Healthcare). Human Hsp90 was first purified from induced *E. coli* cultures using a DEAE column prior to the Ni-NTA affinity purification and gel filtration on S200. Protein was concentrated in 10 mM Tris pH 7.5, 100 mM NaCl using Ultrafree Biomax concentrators (Millipore) to a final concentration of 1–5 mg mL<sup>-1</sup> based on UV<sub>280</sub> absorption. Protein was flash frozen in liquid nitrogen and stored at  $-80^\circ\text{C}$  until use.

### ATPase activity

This assay was adapted from Felts *et al.*<sup>43</sup> 2  $\mu\text{M}$  protein was used in each assay with 1 mM ATP and 0.8  $\mu\text{M}$  [<sup>32</sup>P $\gamma$ ]ATP (6000 Ci mmol<sup>-1</sup>) in solution. For the assays using geldanamycin as a control, a final concentration of 200  $\mu\text{M}$  was used. Twenty minute time points were taken over the course of an hour with the samples shaking and incubating at 37°C. Separation of P<sub>i</sub> from ATP was performed using the thin layer chromatography method described.<sup>43</sup> Visualization of the radiolabeled spots was performed on a Typhoon Imager (GE Healthcare) and quantification was performed using the program ImageQuant (GE Healthcare). The amount of ATP hydrolyzed at each time point was calculated by taking the ratio of P<sub>i</sub> to ATP in solution. This ratio was then multiplied by the total amount of ATP added to the reaction and

normalized by the total protein in solution. A linear fit of the time points gave the rate for each reaction. Activity was plotted on bar graphs using the average of at least three measurements; error bars indicate the standard error of the mean.

### **SAXS data collection and data analysis**

Data reported here was collected at the Advanced Light Source (ALS) beamline 12.3.1 and the Stanford Synchrotron Radiation Laboratory (SSRL) beamline 4.2. To minimize aggregation, samples were spun in a table-top microcentrifuge for 5 min before data collection. SAXS data was collected at 25°C at 2–5 mg mL<sup>-1</sup>. At the ALS, the samples were exposed for 6 and 60 s at a detector distance of 1.6 m. At SSRL samples were exposed for ten 30-s exposures at a detector distance of 2.5 m. Scattering data was recorded on a Mar165CCD detector. The detector channels were converted to  $Q = 4\pi\sin\theta/\lambda$ , where  $2\theta$  is the scattering angle and  $\lambda$  is the wavelength, using a silver behenate sample as a calibration standard. The data was circularly averaged over the detector and normalized by the incident beam intensity. The raw scattering data were scaled and the buffers were subtracted. Individual scattering curves were then merged to provide the final averaged scattering curve. The interatomic distance distribution functions ( $P(r)$ ) were then calculated using the program GNOM.<sup>44</sup>  $D_{\max}$  was determined by constraining  $r_{\min}$  to equal zero and then varying  $r_{\max}$  between 150 and 250 Å.  $R_{\max}$  was then chosen so that the  $P(r)$  curve smoothly approached zero at the upper limit. Small changes in  $r_{\max}$  ( $\pm 10$  Å) did not affect the overall shape of the  $P(r)$  curve. Radii of gyration were calculated from the  $P(r)$ . Comparable results were obtained from the scattering curves using the Guinier approximation as implemented in the program PRIMUS,<sup>44</sup> however the calculated uncertainties were larger due to limitations in the low angle data.

### **Negative-stain electron microscopy**

Purified Hsp90 protein was negatively stained with uranyl formate (pH 5.5–6.0) on thin carbon-layered (40–50 Å thick) 400 mesh copper grids (Pelco) as described.<sup>45</sup> Before staining, protein samples were incubated for 20 min at 150 nM with or without 5 mM AMPPNP (Sigma–Aldrich) at 37°C for *E. coli* and human Hsp90 and 30°C for yeast Hsp90 in 20 mM Tris (pH 7.5), 50 mM KCl, 5 mM MgCl<sub>2</sub>, and 1 mM DTT. Glutaraldehyde (0.005%) crosslinking was performed as described (Southworth and Agard, 2008). Samples were imaged using a Tecnai G2 Spirit TEMs (FEI) operated at 120 keV. Micrograph images were recorded using a 4 k × 4 k CCD camera (Gatan) at 68,000× magnification with 2.2 Å pixel size.

### **Acknowledgments**

The authors thank the entirety of the Agard Lab for many helpful discussions and comments.

### **References**

1. Young JC, Agashe VR, Siegers K, Hartl FU (2004) Pathways of chaperone-mediated protein folding in the cytosol. *Nat Rev Mol Cell Biol* 5:781–791.
2. Freeman BC, Yamamoto KR (2002) Disassembly of transcriptional regulatory complexes by molecular chaperones. *Science* 296:2232–2235.
3. Picard D (2002) Heat-shock protein 90, a chaperone for folding and regulation. *Cell Mol Life Sci* 59:1640–1648.
4. Pratt WB, Toft DO (2003) Regulation of signaling protein function and trafficking by the hsp90/hsp70-based chaperone machinery. *Exp Biol Med* 228: 111–133.
5. Richter K, Muschler P, Hainzl O, Buchner J (2001) Coordinated ATP hydrolysis by the Hsp90 dimer. *J Biol Chem* 276:33689–33696.
6. Young JC, Moaerfi I, Hartl FU (2001) Hsp90: a specialized but essential protein-folding tool. *J Cell Biol* 154: 267–273.
7. Zhao R, Davey M, Hsu YC, Kaplanek P, Tong A, Parsons AB, Krogan N, Cagney G, Mai D, Greenblatt J, Boone C, Emili A, Houry WA (2005) Navigating the chaperone network: an integrative map of physical and genetic interactions mediated by the hsp90 chaperone. *Cell* 120:715–727.
8. Young JC, Hoogenraad NJ, Hartl FU (2003) Molecular chaperones Hsp90 and Hsp70 deliver preproteins to the mitochondrial import receptor Tom70. *Cell* 112: 41–50.
9. Pearl LH, Prodromou C (2006) Structure and mechanism of the hsp90 molecular chaperone machinery. *Annu Rev Biochem* 75:271–294.
10. McClellan AJ, Xia Y, Deutschbauer AM, Davis RW, Gerstein M, Frydman J (2007) Diverse cellular functions of the hsp90 molecular chaperone uncovered using systems approaches. *Cell* 131:121–135.
11. Neckers L, Neckers K (2005) Heat-shock protein 90 inhibitors as novel cancer chemotherapeutics—an update. *Expert Opin Emerg Drugs* 10:137–149.
12. Sharp S, Workman P (2006) Inhibitors of the HSP90 molecular chaperone: current status. *Adv Cancer Res* 95:323–348.
13. Jez JM, Chen JC, Rastelli G, Stroud RM, Santi DV (2003) Crystal structure and molecular modeling of 17-DMAG in complex with human Hsp90. *Chem Biol* 10: 361–368.
14. Roe SM, Prodromou C, O'Brien R, Ladbury JE, Piper PW, Pearl LH (1999) Structural basis for inhibition of the Hsp90 molecular chaperone by the antitumor antibiotics radicicol and geldanamycin. *J Med Chem* 42: 260–266.
15. Obermann WM, Sondermann H, Russo AA, Pavletich NP, Hartl FU (1998) In vivo function of Hsp90 is dependent on ATP binding and ATP hydrolysis. *J Cell Biol* 143:901–910.
16. Hawle P, Siepmann M, Harst A, Siderius M, Reusch HP, Obermann WM (2006) The middle domain of Hsp90 acts as a discriminator between different types of client proteins. *Mol Cell Biol* 26:8385–8395.
17. Prodromou C, Roe SM, O'Brien R, Ladbury JE, Piper PW, Pearl LH (1997) Identification and structural characterization of the ATP/ADP-binding site in the Hsp90 molecular chaperone. *Cell* 90:65–75.

18. Harris SF, Shiau AK, Agard DA (2004) The crystal structure of the carboxy-terminal dimerization domain of htpG, the *Escherichia coli* Hsp90, reveals a potential substrate binding site. *Structure* 12:1087–1097.
19. Meyer P, Prodromou C, Hu B, Vaughan C, Roe SM, Panaretou B, Piper PW, Pearl LH (2003) Structural and functional analysis of the middle segment of hsp90: implications for ATP hydrolysis and client protein and cochaperone interactions. *Mol Cell* 11: 647–658.
20. Meyer P, Prodromou C, Liao C, Hu B, Mark Roe S, Vaughan CK, Vlastic I, Panaretou B, Piper PW, Pearl LH (2004) Structural basis for recruitment of the ATPase activator Aha1 to the Hsp90 chaperone machinery. *EMBO J* 23:511–519.
21. Dutta R, Inouye M (2000) GHKL, an emergent ATPase/kinase superfamily. *Trends Biochem Sci* 25:24–28.
22. Prodromou C, Roe SM, Piper PW, Pearl LH (1997) A molecular clamp in the crystal structure of the N-terminal domain of the yeast Hsp90 chaperone. *Nat Struct Biol* 4:477–482.
23. Panaretou B, Prodromou C, Roe SM, O'Brien R, Ladbury JE, Piper PW, Pearl LH (1998) ATP binding and hydrolysis are essential to the function of the Hsp90 molecular chaperone in vivo. *EMBO J* 17:4829–4836.
24. Shiau AK, Harris SF, Southworth DR, Agard DA (2006) Structural analysis of *E. coli* hsp90 reveals dramatic nucleotide-dependent conformational rearrangements. *Cell* 127:329–340.
25. Ali MM, Roe SM, Vaughan CK, Meyer P, Panaretou B, Piper PW, Prodromou C, Pearl LH (2006) Crystal structure of an Hsp90-nucleotide-p23/Sba1 closed chaperone complex. *Nature* 440:1013–1017.
26. Southworth DR, Agard DA (2008) Species-dependent ensembles of conserved conformational states define the Hsp90 chaperone ATPase cycle. *Mol Cell* 32: 631–640.
27. Krukenberg KA, Forster F, Rice LM, Sali A, Agard DA (2008) Multiple conformations of *E. coli* Hsp90 in solution: insights into the conformational dynamics of Hsp90. *Structure* 16:755–765.
28. Mickler M, Hessling M, Ratzke C, Buchner J, Hugel T (2009) The large conformational changes of Hsp90 are only weakly coupled to ATP hydrolysis. *Nat Struct Mol Biol* 16:281–286.
29. McLaughlin SH, Smith HW, Jackson SE (2002) Stimulation of the weak ATPase activity of human hsp90 by a client protein. *J Mol Biol* 315:787–798.
30. Street TO, Lavery LA, Agard DA (2011) Substrate binding drives large-scale conformational changes in the Hsp90 molecular chaperone. *Mol Cell* 42:96–105.
31. Motojima-Miyazaki Y, Yoshida M, Motojima F (2010) Ribosomal protein L2 associates with *E. coli* HtpG and activates its ATPase activity. *Biochem Biophys Res Commun* 400:241–245.
32. Hessling M, Richter K, Buchner J (2009) Dissection of the ATP-induced conformational cycle of the molecular chaperone Hsp90. *Nat Struct Mol Biol* 16:287–293.
33. Ban C, Junop M, Yang W (1999) Transformation of MutL by ATP binding and hydrolysis: a switch in DNA mismatch repair. *Cell* 97:85–97.
34. Ban C, Yang W (1998) Crystal structure and ATPase activity of MutL: implications for DNA repair and mutagenesis. *Cell* 95:541–552.
35. Corbett KD, Berger JM (2005) Structural dissection of ATP turnover in the prototypical GHL ATPase TopoVI. *Structure* 13:873–882.
36. Cunningham CN, Krukenberg KA, Agard DA (2008) Intra- and intermonomer interactions are required to synergistically facilitate ATP hydrolysis in Hsp90. *J Biol Chem* 283:21170–21178.
37. McLaughlin SH, Ventouras LA, Lobbezoo B, Jackson SE (2004) Independent ATPase activity of Hsp90 subunits creates a flexible assembly platform. *J Mol Biol* 344:813–826.
38. Vasko R, Rodriguez R, Cunningham C, Ardi V, Agard D, McAlpine S (2010) Mechanistic studies of sansalvamide A-amide: an allosteric modulator of Hsp90. *ACS Med Chem Lett* 1:4–8.
39. Alexander LD, Partridge JR, Agard DA, McAlpine SR (2011) A small molecule that preferentially binds the closed conformation of Hsp90. *Bioorg Med Chem Lett* 21:7068–7071.
40. Dollins DE, Warren JJ, Immormino RM, Gewirth DT (2007) Structures of GRP94-nucleotide complexes reveal mechanistic differences between the hsp90 chaperones. *Mol Cell* 28:41–56.
41. Huai Q, Wang H, Liu Y, Kim HY, Toft D, Ke H (2005) Structures of the N-terminal and middle domains of *E. coli* Hsp90 and conformation changes upon ADP binding. *Structure* 13:579–590.
42. Southworth DR, Agard DA (2011) Client-loading conformation of the Hsp90 molecular chaperone revealed in the cryo-EM structure of the human Hsp90:Hop complex. *Mol Cell* 42:771–781.
43. Felts SJ, Owen BA, Nguyen P, Trepel J, Donner DB, Toft DO (2000) The hsp90-related protein TRAP1 is a mitochondrial protein with distinct functional properties. *J Biol Chem* 275:3305–3312.
44. Konarev PV, Volkov VV, Sokolova AV, Koch MHJ, Svergun DI (2003) PRIMUS: a Windows PC-based system for small-angle scattering data analysis. *J Appl Cryst* 36:1277–1282.
45. Ohi M, Li Y, Cheng Y, Walz T (2004) Negative staining and image classification—powerful tools in modern electron microscopy. *Biol Proced Online* 6:23–34.